Pergamon

Journal of Structural Geology, Vol. 18, No. 5, pp. 615 to 623, 1996
Copyright © 1996 Elsevier Science Ltd
Printed in Great Britain. All rights reserved
0191-8141/96 $15.00+0.00

0191-8141(95)00104-2

Contrasting roles of detrital and authigenic phyllosilicates during slaty cleavage development

NEI-CHE HO, DONALD R. PEACOR and BEN A. VAN DER PLUIJM

Department of Geological Sciences, University of Michigan, 2534 C.C. Little Building, Ann Arbor, MI 48109-1063, U.S.A.

(*Received* 28 *March* 1995; *accepted in revised form* 22 *August* 1995)

Abstract—Eight samples from a prograde slate sequence from Central Wales, ranging from the diagenetic zone to the epizone, were studied by X-ray texture goniometry, SEM and TEM. X-ray pole figure data imply that, in the four lower-grade samples, the crystallographic preferred orientations of both mica and chlorite change from parallel to bedding, to intermediate to bedding and cleavage, to parallel to cleavage orientation with increasing grade. There is no difference in the degree of preferred orientation between mica and chlorite in individual samples. The sample with an intermediate preferred orientation has the lowest degree of preferred orientation. In the four higher-grade samples, the preferred orientations of mica are primarily in the cleavage orientation, whereas those of chlorite are largely parallel to bedding.

Observations by SEM and TEM show that the samples have two populations of phyllosilicates: (1) large (tens of μm) chlorite–mica stacks of detrital origin, dominated by chlorite in a matrix of (2) authigenic fine-grained (tens of nm) mica and chlorite with dominant illite (muscovite). Preferred orientation measurements of chlorite primarily reflect the chlorite in the stacks. However, preferred orientation measurements of mica are dominated by the mica in the stacks for four lower-grade samples, but by mica in the fine-grained matrix with (001) parallel to cleavage for the four higher-grade samples. These observations collectively show that: (1) mechanical rotation of detrital grains was the dominant reorientation mechanism of cleavage formation in the lower-grade samples; (2) in the higher-grade samples, the preferred orientation of matrix mica and chlorite transformed from bedding-parallel to cleavage-parallel primarily by dissolution and neo-crystallization. Copyright © 1996 Elsevier Science Ltd

INTRODUCTION

The importance of crystallographic preferred orientation development of phyllosilicates in deformed rocks, particularly of chlorite and mica, has been the subject of many studies. It has been used, for example, to investigate the processes and mechanisms of cleavage development (e.g. Holeywell and Tullis 1975, Ho *et al.* 1995) and to estimate finite strain (e.g. Tullis & Wood 1975, Chen & Oertel 1980, Oertel *et al.* 1989). Crystallographic preferred orientation of large numbers of grains can be conveniently determined by means of X-ray texture goniometry (Schulz 1949, Wenk 1985). The X-ray technique of measuring preferred orientation of phyllosilicates has been optimized through the years (e.g. Lipshie *et al.* 1976, Oertel 1983, van der Pluijm *et al.* 1994). In the case of phyllosilicates, the crystallographic preferred orientation also represents the dimensional preferred orientation, and shape plays a significant role in the reorientation processes (e.g. Hobbs *et al.* 1976, p. 249, Knipe 1981, van der Pluijm & Kaars-Sijpesteijn 1984). Nevertheless, because X-ray goniometry measures crystallographic properties, the term 'crystallographic preferred orientation' is preferred over dimensional preferred orientation in this paper.

In past X-ray goniometry studies of slates, little attention has been paid to distinguishing the contributions of phyllosilicates of different origins (i.e. detrital vs authigenic phases). Recent studies (e.g. Li *et al.* 1993, Ho *et al.* 1995) showed that phyllosilicates in the fine-grained matrix, predominantly of authigenic origin and with crystal thicknesses in the range of tens of nm, may behave differently from detrital grains, which generally have large sizes (on the order of tens of μm). Detrital phyllosilicate grains may occur as chlorite–mica stacks that are oriented with basal planes and long dimensions parallel or subparallel to bedding, and which are commonly markedly deformed. In contrast, matrix phyllosilicates consist predominantly of fine-grained authigenic white mica and chlorite, commonly with (001) planes oriented parallel to either bedding or cleavage. Because phyllosilicates of different origins may display different responses to deformation, it is important to identify their respective contributions to the bulk crystallographic orientation data that are integrated by X-ray diffraction over all grains of a given mineral regardless of origin, and to determine the respective deformation mechanisms during cleavage development. Direct observations of the rock fabric with scanning electron microscopy (SEM) and transmission electron microscopy (TEM) provide complementary information for interpreting the crystallographic preferred orientation data obtained by X-ray texture goniometry. However, SEM is mainly able to resolve those large phyllosilicates that are primarily detrital in origin (e.g. stacks), and authigenic phases can only be identified on the TEM scale. Thus, each of these imaging techniques provides incomplete characterization of the samples. X-ray texture goniometry, on the other hand, obtains data from all the minerals present, regardless of their sizes and origin, dependent only on the volume of grains in a particular orientation. Therefore, X-ray texture gonio-

metry data can only be correctly interpreted if corresponding SEM and TEM results are included. By integrating results from these techniques, the aim of this study is to determine the contributions of phyllosilicates of different origin to X-ray crystallographic preferred orientation, and the dominant deformation mechanism during cleavage development as a function of metamorphic grade, over a range from the diagenetic zone to the epizone.

GEOLOGICAL SETTING AND SAMPLING

The study area is located in the Rhayader district of the central Welsh Basin (Fig. 1, inset). The Lower Paleozoic rocks of the Welsh Basin have been the subject of several studies in characterizing regional low-grade metamorphism. Merriman *et al.* (1992) carried out a detailed white mica crystallinity survey in the Rhayader district, using a sampling density of approximately one mudrock per 1.5 km^2, and generated a contoured white mica crystallinity map (Fig. 1).

White mica crystallinity (also known as illite crystallinity), generally expressed as °$\Delta 2\theta$CuKα, is essentially a measure of the half-height width of the 10-Å X-ray diffraction peak of the <2 μm fraction (Kubler 1967), and has been shown to be primarily a function of illite crystallite size and crystal imperfection density (e.g. Árkai & Tóth 1983, Peacor 1992, Jiang 1993). The technique for measuring illite crystallinity has been standardized by Kisch (1990). Using illite crystallinity, the very-low- to low-grade metamorphic regime can be sub-divided into three zones, from low to high grade: diagenetic zone (>0.42°$\Delta 2\theta$ CuKα); anchizone; and epizone (<0.25°$\Delta 2\theta$ CuKα). These terms, applied to pelitic rocks, can be roughly correlated with the zeolite, prehnite–pumpellyite and greenschist facies as defined for metabasites. The dominant factor in determining half-height width of the illite 10-Å peak is the broadening effect of small crystallite size (Merriman *et al.* 1990). Therefore, smaller illite crystallinity values correspond to larger average illite crystallite sizes and higher grades.

The contoured map of Fig. 1 shows a pattern of regional metamorphism that is broadly characterized by increasing grade toward the northwest. Eight oriented samples with mesoscopically discernible bedding and cleavage were collected to represent the range of grade from the diagenetic zone to the epizone (Table 1). Sample locations and corresponding illite crystallinity data are shown in Figs. 1 and 2. The shales and slates generally consist of μm- to mm-sized grains of quartz, albite, white mica and chlorite–mica stacks having the characteristics of detrital grains, in a phyllosilicate matrix of intergrown fine-grained chlorite and white mica (Merriman *et al.* 1992). Chlorite–mica stacks may

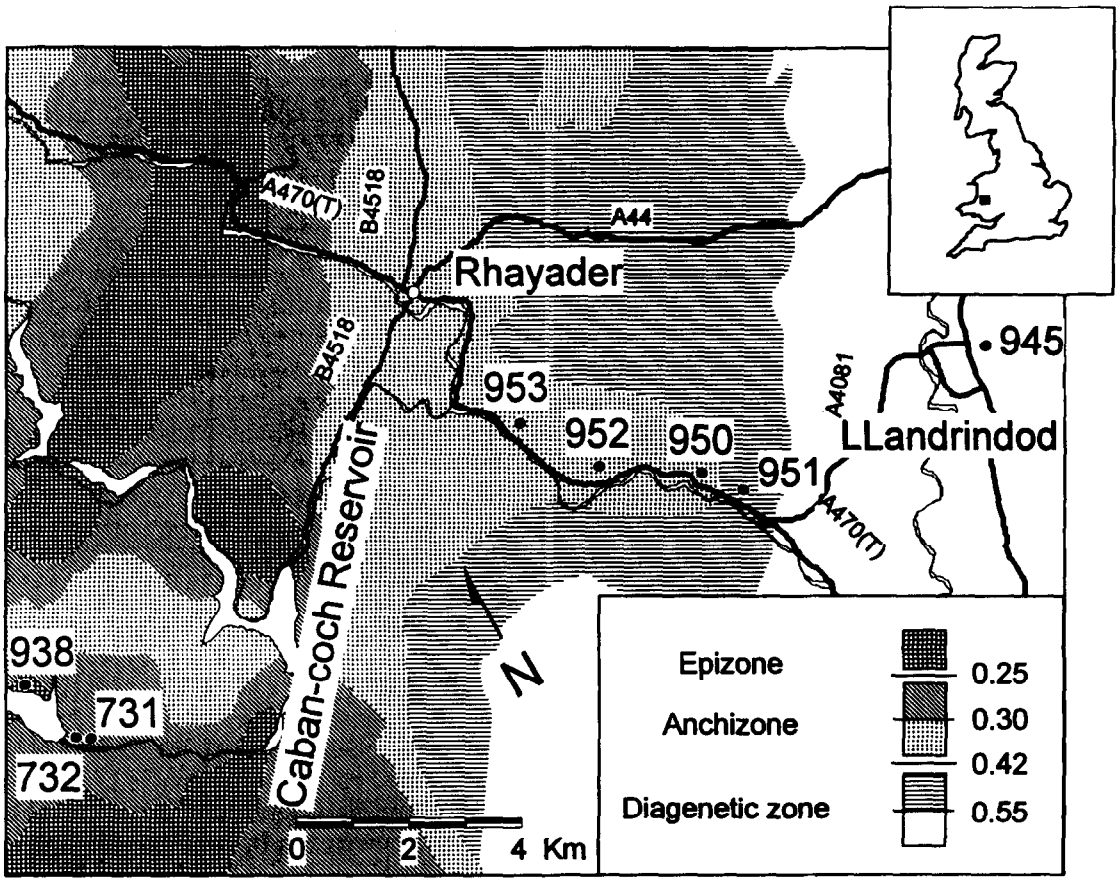

Fig. 1. Location map, showing contoured illite crystallinity data (after Merriman *et al.* 1992). Sample numbers and corresponding localities are shown.

Table 1. Illite crystallinity and maximum value and contour interval for projections in Fig. 2

Sample ID	IC °Δ2θ	Grade	Chlorite (001) Max	Chlorite (001) Contour interval	Mica (001) Max	Mica (001) Contour interval
BRM 945	0.54	Diagenetic	5.86	0.6	6.15	0.6
BRM 951	0.45	Diagenetic	2.50	0.2	2.38	0.2
BRM 950	0.41	Low anchizone	5.14	0.6	5.18	0.6
BRM 952	0.39	Low anchizone	5.51	0.6	5.66	0.6
BRM 953	0.37	Low anchizone	5.20	0.8	3.73	0.6
BRM 731	0.29	High anchizone	5.94	0.6	3.76	0.6
BRM 732	0.26	High anchizone	5.43	0.4	3.74	0.4
BRM 938	0.23	Epizone	4.99	0.6	6.21	0.6

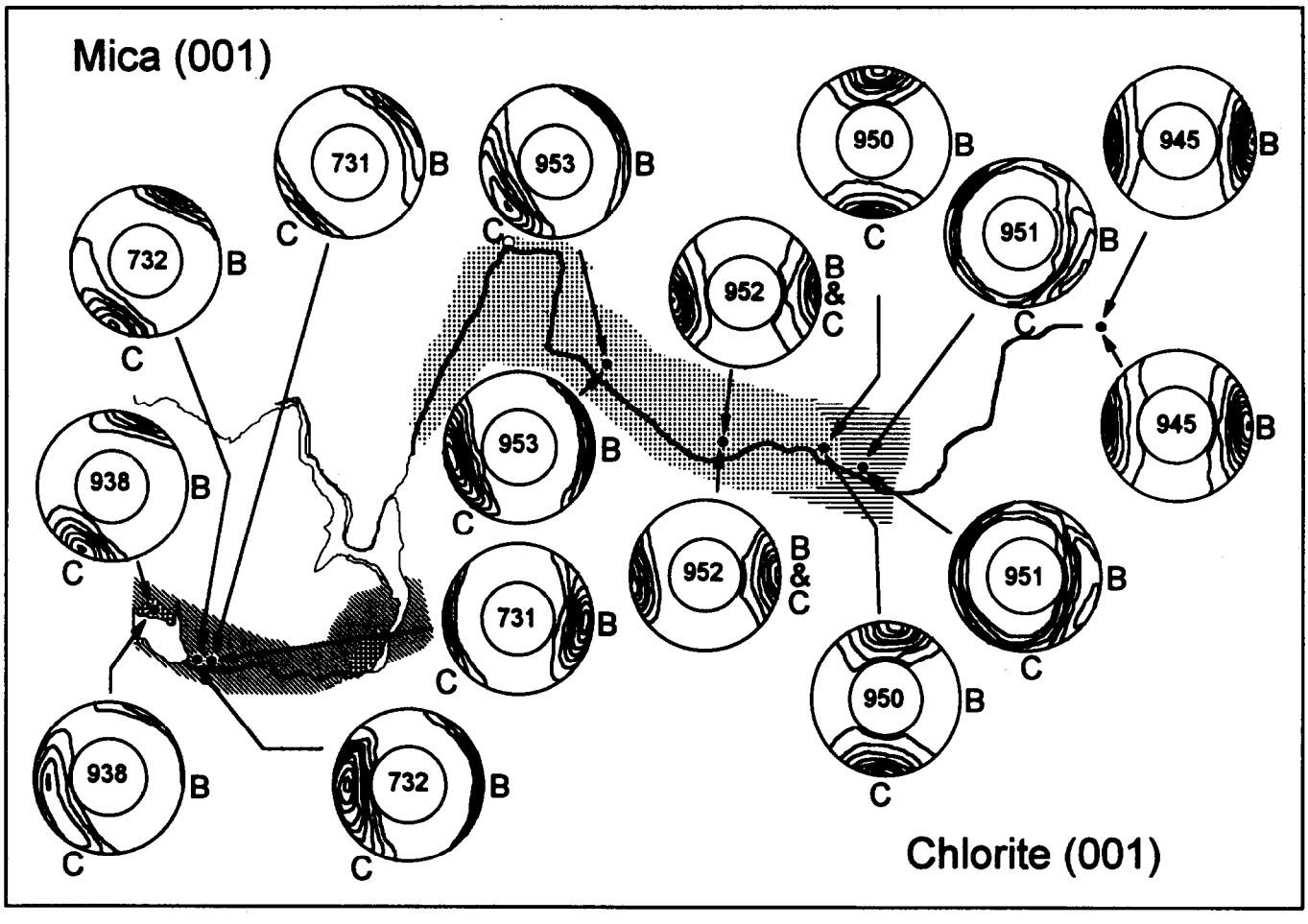

Fig. 2. Lower-hemisphere equal-area projections of mica (001) (upper row) and chlorite (001) (lower row) orientations. Poles to bedding and cleavage are labeled as B and C, respectively. Due to the angular limitation of the transmission mode for one sample section, data are not obtained in the center area of the projections. Plots are contoured in multiples of random distribution (m.r.d.). The maximum intensity and the contour interval for each sample are listed in Table 2.

comprise up to 50% of some samples, having developed by replacement of detrital grains of mafic minerals, primarily biotite, through a series of textural and compositional changes in response to diagenesis and low-grade metamorphism (Li *et al.* 1994).

Sample BRM 945 (diagenetic zone) is the only sample in which no cleavage is present in hand specimen; however, the specimen splits along the bedding plane. The quality of mesoscopic cleavage improves as grade increases (to the northwest). Samples from the high-anchizone and epizone show well-developed cleavage.

METHODS OF STUDY AND SAMPLE PREPARATION

The crystallographic preferred orientation measurements were performed on a modified X-ray pole figure device attached to an Enraf–Nonius CAD4 single-crystal diffractometer equipped with a Mo source. The detailed instrumentation and correction procedures have been described in van der Pluijm *et al.* (1994). For observing the internal structure of samples and features within component crystals, a Hitachi S-570 scanning

electron microscope (SEM) and a Philips CM 12 scanning transmission electron microscope (STEM), both equipped with Kevex Quantum energy dispersive spectral (EDS) analysis systems, were used.

Polished slabs *ca* 0.2 mm (200 μm) thick were used for X-ray texture analysis. Thin sections of standard thickness with high-quality diamond-polished surfaces were used for SEM observations. For TEM work, specimens were removed from sticky-wax-backed thin sections, and then ion-milled. Therefore, three parallel thin sections, each perpendicular to the line of intersection of bedding and cleavage, were sequentially made from each hand sample. From these sections, specimens for X-ray texture goniometry and EM work were made following the procedures in van der Pluijm *et al.* (1994) and Jiang and Peacor (1991), respectively.

The measured X-ray intensities are first corrected for background and absorption. The corrected intensities, then, are normalized and expressed in multiples of a random distribution (m.r.d.), which is equivalent to percentage per 1% area (Wenk, 1985). Although only three-quarters of the area of a complete pole figure is measured in one measurement, intensities are still normalized against whole area since the intensity contribution from the not-measured area is negligible. The pole figures shown in this paper are all lower-hemisphere equal-area projection.

RESULTS

X-ray texture goniometry data

The X-ray texture goniometry data are shown in Fig. 2. The road indicated in the center of the figure serves as a reference (cf. Fig. 1), and the illite crystallinity values of each sample are given next to their localities. The data are presented as contoured X-ray intensity data on the lower-hemisphere projection, and on the plane orthogonal to bedding and cleavage. The letter 'B' marks the position of the pole to the bedding, and the letter 'C' the position of the pole to cleavage. Maximum intensities and contour intervals for each sample are listed in Table 1. All data have been rotated so that the bedding orientation is standardized as 'east', regardless of its orientation in each outcrop. The diagrams in the upper row are for the mica (001) reflection (10-Å peak), and in the lower row are for the chlorite (001) reflection (14-Å peak).

The preferred orientation of mica in the sample of the lowest grade (BRM 945, 0.54°$\Delta 2\theta$ CuKα) is in the bedding orientation. As the cleavage develops and the grade increases, it changes to an orientation intermediate to those of bedding and cleavage (BRM 951, 0.45°$\Delta 2\theta$ CuKα), and subsequently to being parallel to cleavage (BRM 950, 0.41°$\Delta 2\theta$ CuKα and BRM 952, 0.39°$\Delta 2\theta$ CuKα). Cleavage in sample BRM 952 is parallel to bedding, but bedding and cleavage have different orientations in all other samples. In higher grade samples, the preferred orientation of mica is always parallel to the cleavage. Asymmetric patterns with a tail towards the bedding pole are visible in the pole figures of samples 953, 731 and 732.

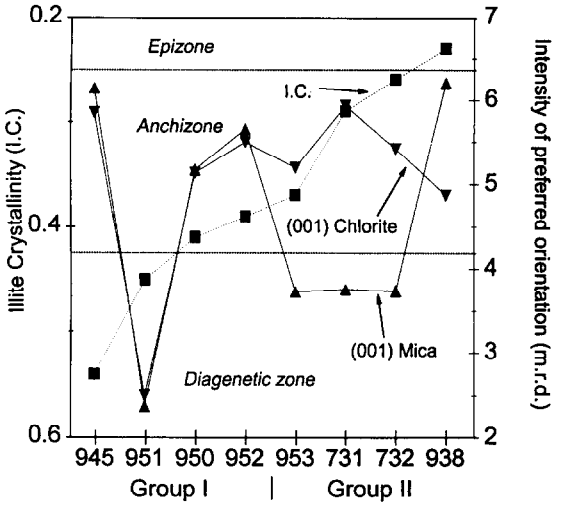

Fig. 3. Intensity of preferred orientation (in m.r.d.) based on pole figures for each sample plotted as a function of illite crystallinity grade; illite crystallinity values are separately plotted. Data are listed in Table 1.

The preferred orientation of chlorite shows a different pattern. The trend in orientation is the same as that of mica in the four lower-grade samples. It is parallel to bedding in the lowest-grade sample (BRM 945, 0.54°$\Delta 2\theta$ CuKα), changing to an orientation intermediate to bedding and cleavage (BRM 951, 0.45°$\Delta 2\theta$ CuKα), and then parallel to cleavage (BRM 950, 0.41°$\Delta 2\theta$ CuKα and BRM 952, 0.39°$\Delta 2\theta$ CuKα). However, in the four samples of higher grade, the chlorite preferred orientation is parallel to bedding. Similar to the mica pole figures, asymmetric patterns are also visible in the pole figures of samples 953,731 and 732, but with a tail towards the cleavage pole.

The intensities of preferred orientation, expressed in m.r.d., are listed in Table 1 and plotted in Fig. 3. The corresponding illite crystallinity values are also plotted in this figure. For each sample, several sets of data were measured, but only one set of data, corresponding to the figure shown in Fig. 2, is listed. Intensity values in different sets differ by no more than 15%. For the lower-grade samples, in which the preferred orientations of mica and chlorite lie in the same direction (945, 951, 950 and 952), the degress of preferred orientation are nearly identical. The minimum value occurs in the sample with

Fig. 4. Selected images of low-grade samples from group I: (a) BRM 945 (SEM); (b) BRM 945 (TEM); (c) BRM 951 (SEM); and (d) BRM 950 (SEM). Mica (M), chlorite (Chl), mica–chlorite stacks (M–C) and quartz (Q) are labelled in (c); minerals can be identified in the other images as they display the same contrast as in (c). Bedding and cleavage directions are indicated by arrows. Scale bar is shown in each photograph.

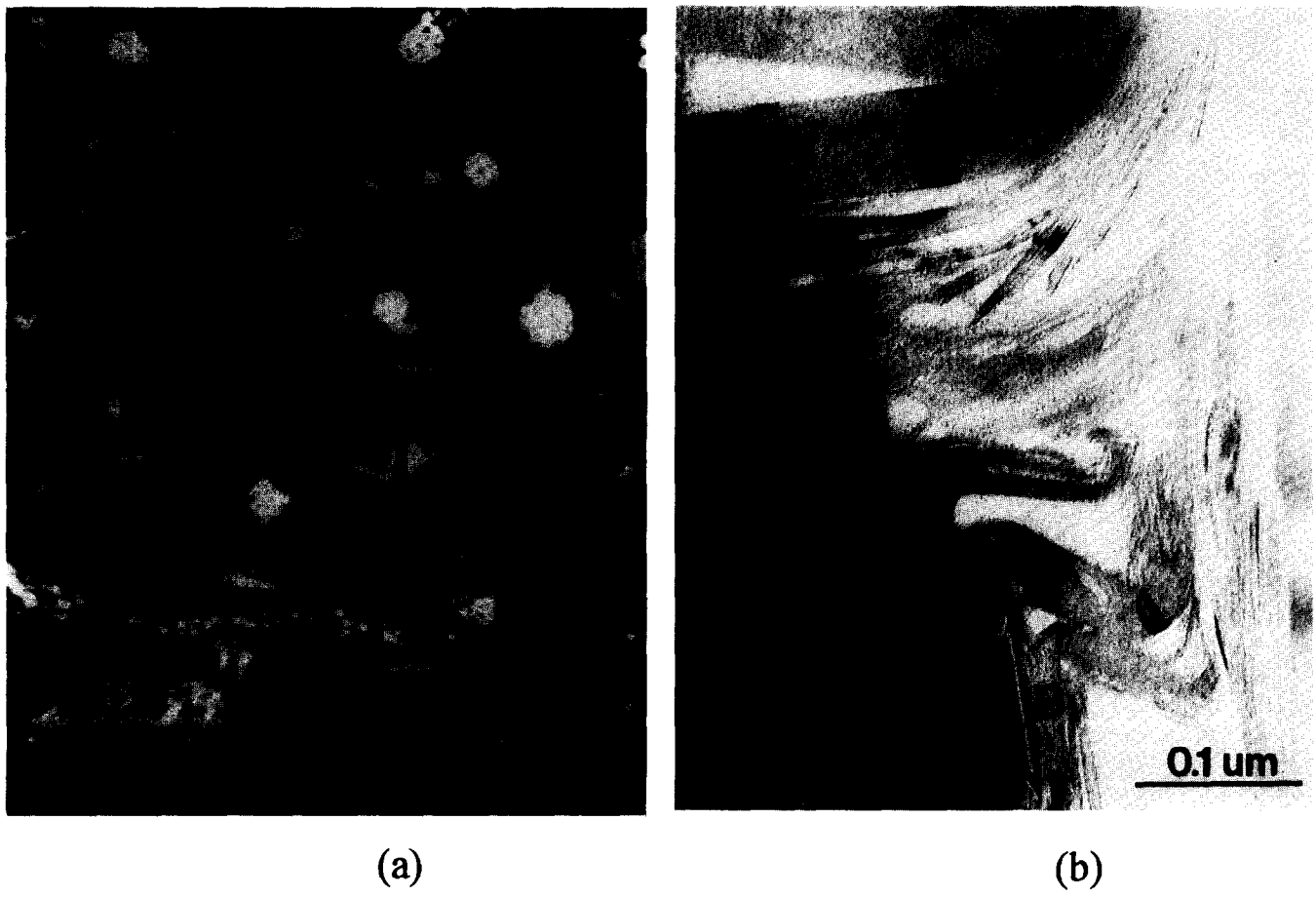

Fig. 4.

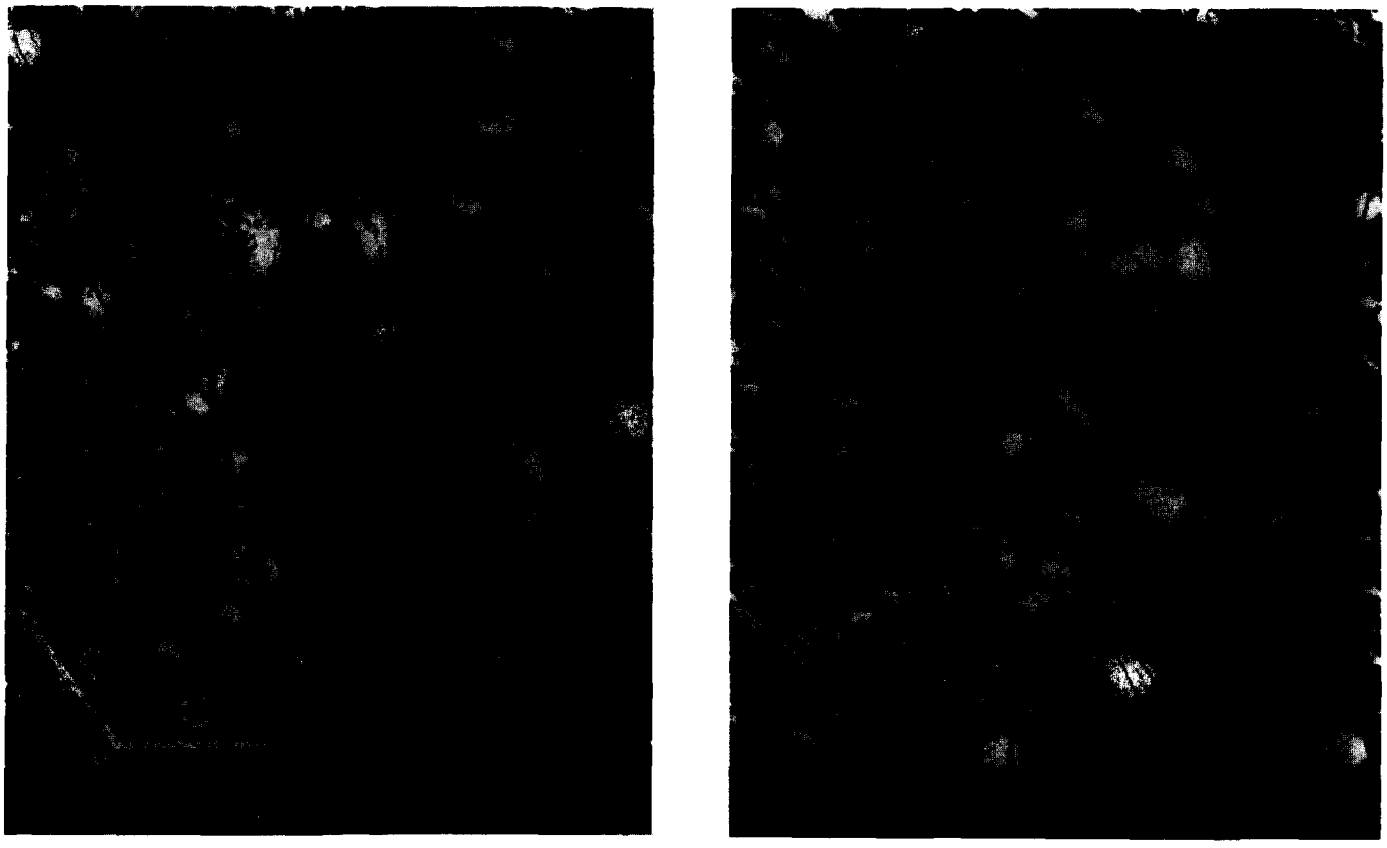

(a) (b)

(c)

Fig. 5.

the preferred orientations intermediate to bedding and cleavage (BRM 951). For the higher-grade samples, the degree of preferred orientation of mica, which is oriented preferentially parallel to cleavage, is generally less than that of chlorite, which is oriented parallel to bedding. The degree of preferred orientation of mica is greater than that of chlorite only in the highest-grade sample (BRM 938). There seems to be a significant increase in degree of preferred orientation in mica and a small decrease for chlorite in samples with grade higher than that of BRM 732. However, because of the limited amount of data, these latter trends remain uncertain.

SEM and TEM observations

All SEM images shown were obtained in backscattered electron (BSE) mode. In this mode, because of the difference in composition, mica and chlorite can be distinguished by their contrast, with chlorite brighter than mica. The textural relations for mica, chlorite and chlorite–mica stacks are shown in Fig. 4. The width of view of most of the SEM photographs is ~0.5–1 mm, which is approximately equal to the 1 mm diameter of the X-ray beam used for measuring preferred orientation data. Therefore, the areas represented by SEM images correspond to the areas analyzed by the X-ray texture goniometry.

Two modes of occurrence of phyllosilicates were observed in SEM and TEM: (1) large μm-sized chlorite–mica stacks, dominated by chlorite. We refer to this kind of larger grain, easily resolvable in the lower-resolution SEM images, as detrital in origin, as previous work indicates that such chlorite–mica stacks were originally detrital biotite grains that were modified, in part by replacement of biotite by chlorite during diagenesis and metamorphism (e.g. Li *et al.* 1994); (2) fine-grained mica and chlorite with dominant illite (muscovite) (Fig. 4b). The thickness of each phyllosilicate packet is on the order of 0.02 μm, which is too small to be resolved in SEM images. This kind of phyllosilicate, comprising the fine-grained matrix, is authigenic in origin (Merriman *et al.* 1990, Li *et al.* 1994). Individual crystals are only resolvable at the high-resolution TEM scale.

In the lowest-grade sample (BRM 945, Fig. 4a), a preferred orientation parallel to bedding is well defined by the basal planes of detrital phyllosilicates observed in the SEM image. However, a range of orientations can be observed in the TEM image (Fig. 4b) of authigenic clays. Detrital phyllosilicates in sample BRM 951 (Fig. 4c) have a variety of orientations, and show abundant deformation features. An apparent preferred orientation can not be directly determined from this image. Nevertheless, it is clear that the average preferred orientation would be intermediate to the bedding and cleavage orientations. The presence of thin bands of phyllosilicates parallel or sub-parallel to the cleavage, sometimes containing small euhedral crystals, suggest that cleavage is determined by a dissolution–neocrystallization process. In sample BRM 950 (low anchizone, Fig. 4d), the majority of grains are parallel to cleavage, although a few detrital grains remain aligned parallel to bedding.

Figure 5(a) (BRM 731, high anchizone) and Fig. 5(b) (BRM 938, epizone) are representative SEM images of higher-grade samples. In both images, a preferred orientation parallel to bedding can be recognized from the alignment of the (001) planes of chlorite–mica stacks, especially the stacks of larger size. A weak preferred orientation parallel to cleavage, formed by the alignment of (001) of a number of smaller stacks and mica grains, can be seen in Fig. 5(b) (BRM 938). Deformation of individual grains is common, and minerals in the cleavage orientation often cross-cut grains in other orientations.

The collective SEM observations show that both chlorite and mica occur in chlorite–mica stacks, but with chlorite being the dominant phase (e.g. significantly larger proportion of bright areas relative to gray areas in BSE images). Individual detrital mica or chlorite grains are observed in only a few cases (e.g. Figs. 5a & b).

Mica was more frequently encountered than chlorite in TEM images, suggesting that mica is the dominant phase of the matrix materials. It is difficult to determine representative preferred orientations of mica and chlorite from TEM images for lower-grade samples because of the large range of small packet orientations within the small image areas. However, as grade increases, better aligned and thicker phyllosilicate packets occur in the cleavage orientation, suggesting preferred orientation development in the cleavage orientation. Moreover, these thicker, essentially strain-free packets in the cleavage orientation are often seen to cross-cut grains in other orientations (Fig. 5c), further supporting a dissolution–neocrystallization origin for cleavage-parallel phyllosilicates.

DISCUSSION AND CONCLUSIONS

For discussion purposes, the prograde sequence is subdivided into two groups, based on characteristics of the X-ray analysis data. Group I consists of samples in which the crystallographic preferred orientations of mica and chlorite are similar (945, 951, 950 and 952), but this common orientation changes from parallel to bedding in the lowest-grade sample, to intermediate to bedding and cleavage, and then to parallel to cleavage. Group II contains the remaining samples (953, 731, 732

Fig. 5. Selected images of high-grade samples from sample II: (a) BRM 731 (SEM); (b) BRM 938 (SEM); and (c) TEM image from BRM 938. Minerals can be identified by the same contrast as in Fig. 4. Bedding and cleavage directions and scale bar are shown in each photograph.

and 938). In group II samples, the X-ray crystallographic preferred orientation of mica is mainly parallel to cleavage. However, the X-ray crystallographic preferred orientation of chlorite is mainly parallel to the bedding orientation. Group I samples represent the lower-grade portion (diagenetic–low anchizone) of the continuous pro-grade metamorphic sequence, whereas those of group II represent the higher-grade range (low anchizone–epizone).

As concluded from SEM observations for group I, the alignment of the (001) planes of detrital phyllosilicates (detrital mica in BRM 945, chlorite–mica stacks in other samples) are parallel to bedding (945), intermediate to bedding and cleavage (951), and parallel to cleavage (950). In group II, basal planes of detrital phyllosilicate are essentially parallel to bedding for all samples. For chlorite, the X-ray crystallographic preferred orientation data correlate with the preferred orientations of detrital phyllosilicates as shown by SEM observations for all samples. Thus, it appears that the crystallographic preferred orientation of chlorite is dominated by chlorite in chlorite–mica stacks for all samples, regardless of their metamorphic grade.

The situation, however, is different for mica. In group I samples, the X-ray crystallographic preferred orientation of mica is the same as that of chlorite and the preferred orientation of detrital chlorite–mica stacks as suggested by SEM images. TEM observations, on the other hand, show no apparent preferred orientation. Although mica is the dominant phase in the matrix, it will probably not contribute significantly to the overall result because of its relatively random orientation. Therefore, the X-ray crystallographic preferred orientation of mica is likely also dominated by the mica in the detrital phases (as individual grains or within chlorite–mica stacks). In group II samples, the crystallographic preferred orientation of mica is primarily parallel to cleavage, but the basal planes of chlorite–mica stacks, as shown by SEM images, are preferentially aligned parallel to bedding. This suggests that mica in the stacks does not contribute significantly to the X-ray data. On the other hand, TEM observations imply a well-defined preferred orientation in the cleavage direction for authigenic mica. This agreement between X-ray crystallographic preferred orientation data and TEM observations suggests that, in group II samples, mica occurs principally as an authigenic phase, which dominates the crystallographic preferred orientation measurements. These observations collectively suggest that each X-ray pole figure is the sum of the separate preferred orientations of detrital and authigenic phases, as implied by SEM and TEM images, respectively, and that the orientation of the maximum is controlled by the dominant phase. Therefore, we conclude that the preferred orientation of mica is dominated by detrital phases in the lower-grade group I samples, but as grade increases, the contribution of authigenic mica increases and eventually dominates the X-ray measurements.

In addition to showing the differences in contributions to X-ray crystallographic preferred orientation measurements from detrital and authigenic phyllosilicates, this suite of samples also provides an opportunity to study their reorientation mechanisms with changing metamorphic grade. Mechanical rotation and dissolution–neocrystallization are considered end-member processes in cleavage development (e.g. Wood 1974). Geological parameters such as temperature, fluid/rock ratio, the composition of pore fluids, porosity, state of lithification and strain (rate) have all been proposed as significant controlling parameters. Mechanical rotation of grains would create a continuous range in orientations. A crystallographic preferred orientation that is intermediate to those of bedding and cleavage therefore develops, accompanied by an overall decrease in the degree of preferred orientation because of the larger scatter. The degree of preferred orientation should increase again once the preferred orientation of rotated grains or portions thereof are in the cleavage direction. These characteristics agree well with the X-ray texture goniometry data for the low-grade samples from group I for both mica and chlorite. Direct observations of deformation features, as seen in Figs. 4(b) & (c) further imply that mechanical rotation is the dominant mechanism in these low-grade samples.

In contrast, authigenic minerals preferentially crystallize in the cleavage orientation at the expense of minerals dissolving in other orientations as cleavage develops. This would result in a bimodal orientation distribution and a paucity of intermediate orientations between bedding and cleavage, or a slight asymmetry in preferred orientation (Etheridge & Oertel 1979, Sintubin 1994). Samples in group II show that mica has a maximum in the cleavage orientation with a tail towards the bedding orientation, whereas the maximum for chlorite lies in the bedding orientation with a tail towards the cleavage orientation. Moreover, the mica distribution appears to become less asymmetric with increasing grade. These slightly asymmetric patterns indicate that rotation and internal deformation of detrital grains played a minor role in the samples from group II, and that growth of minerals in the cleavage orientation is dominated by dissolution and neocrystallization of mica. This view is supported by large detrital grains that are cross-cut by thin bands of phyllosilicates parallel to the cleavage orientation and thicker, relatively strain-free cleavage-parallel phyllosilicate packets cross-cutting packets in other orientations (Fig. 5c).

In conclusion, X-ray preferred orientations of mica and chlorite combined with data on the metamorphic grade from illite crystallinity measurements, indicate that although both mechanical rotation and dissolution–neocrystallization are active in all samples, mechanical rotation is the dominant process of cleavage formation in the lower-grade regime (group I), and dissolution–neocrystallization is the dominant cleavage formation mechanism in the higher-grade regime (group II).

Acknowledgements—The single-crystal diffractometer was acquired under grant EAR-8917350; the STEM used in this study was acquired under grant EAR-87-08276, and the SEM under grant BSR-83-14092, all from the National Science Foundation. This study was supported by

the American Chemical Society Petroleum Research Fund (Grant 27461-AC8). Special thanks are due to R. J. Merriman (British Geological Survey), who kindly assisted with the field work. Helpful reviews were given by H. Kisch, M. Sintubin, and journal editor J. P. Evans.

REFERENCES

Árkai, P. & Tóth, M. N. 1983. Illite crystallinity; combined effects of domain size and lattice distortion. *Acta Geol. Hungarica* **26**, 341–358.

Bevins, R. E. & Rowbotham, G. 1983. Low-grade metamorphism within the Welsh sector of the paratectonic Caledonides. *Geol. J.* **18**, 141–168.

Chen, R. T. & Oertel, G. 1989. Strain history of the Los Prietos syncline, Santa Maria basin, California: a case of post-tectonic compaction. *J. Struct. Geol.* **11**, 539–551.

Etheridge, M. A. & Oertel, G. 1979. Strain measurements from phyllosilicate preferred orientation—a precautionary note. *Tectonophysics* **60**, 107–120.

Ho, N.-C., Peacor, D. R. & van der Pluijm, B. A. 1995. Reorientation Mechanisms of phyllosilicates in the shale to slate transition at Lehigh Gap, PA. *J. Struct. Geol.* **17**, 345–356.

Holeywell, R. C. & Tullis, T. E. 1975. Mineral reorientation and slaty cleavage in the Martinsburg Formation, Lehigh Gap, Pennsylvania. *Bull. geol. Soc. Am.* **86**, 1296–1304.

Hobbs, B. E., Means, W. D. & Williams, P. F. 1976. *An Outline of Structural Geology*. John Wiley & Sons, New York.

Jiang, W.-T. 1993. Diagenesis and very low-grade metamorphism of pelitic rocks from the Gaspé Peninsula, Québec. Unpublished Ph.D. thesis, University of Michigan.

Jiang, W.-T. & Peacor, D. R. 1991. Transmission electron microscopic study of the kaolinitization of muscovite. *Clays & Clay Miner.* **39**, 1–13.

Kisch, H. J. 1990. Calibration of the anchizone: a critical comparison of illite 'crystallinity' scales used for definition. *J. Metamorph. Geol.* **8**, 31–46.

Knipe, R. J. 1981. The interaction of deformation and metamorphism in slates. *Tectonophysics* **78**, 249–272.

Kubler, B. 1967. La cristallinité de l'illite et les zones tout à fait supérieures du métamorphisme. In: *Etages Tectonique. Colloque à Neuchâtel*. La Baconnière, Neuchâtel, 105–120.

Li, G., Peacor, D. R., Merriman, R. J., Roberts, B. & van der Pluijm, B. A. 1994. TEM and AEM constraints on the origin and significance of chlorite–mica stacks in slates: an example from Central Wales, U.K. *J. Struct. Geol.* **16**, 1139–1157.

Lipshie, S. R., Oertel, G. & Christie, J. M. 1976. Measurement of preferred orientation of phyllosilicates in schists. *Tectonophysics* **34**, 91–99.

Merriman, R. J., Roberts, B. & Peacor, D. R. 1990. A transmission electron microscope study of white mica crystallite size distribution in a mudstone to slate transitional sequence, North Wales, U.K. *Contr. Miner. Petrol.* **106**, 27–40.

Merriman, R. J., Roberts, B. & Hirons, S. R. 1992. Regional low grade metamorphism in the central part of the Lower Paleozoic Welsh Basin: an account of the Llanilar and Rhayader districts, BGS 1:50K sheets 178 & 179. British Geological Survey Technical Report, WG/91/16.

Oertel, G., Engelder, T. & Evans, K. 1989. A comparison of the strain of crinoid columnals with that of their enclosing silty and shaly matrix on the Appalachian Plateau, New York. *J. Struct. Geol.* **11**, 975–993.

Oertel, G. 1983. The relationship of strain and preferred orientation of phyllosilicate grains in rocks—a review. *Tectonophysics* **100**, 413–447.

Peacor, D. R. 1992. Diagenesis and low grade metamorphism of shale and slates. In: *Minerals and Reactions at the Atomic Scale: Transmission Electron Microscopy* (Edited by Buseck, P.R.). Mineralogical Society of America, Washington, DC, 335–380.

Schulz, L. G. 1949. A direct method for determining preferred orientation of a flat reflection sample using a Geiger counter X-ray spectrometer. *J. appl. Phys.* **20**, 1033–1036.

Sintubin, M. 1994. Phyllosilicate preferred orientation in relation to strain path determination in the lower Paleozoic Stavelot–Venn Massif (Ardennes, Belgium). *Tectonophysics* **237**, 215–231.

Tullis, T. E. & Wood, D. S. 1975. Correlation of finite strain from both reduction bodies and preferred orientation of mica in slate from Wales. *Bull. geol. Soc. Am.* **86**, 632–638.

van der Pluijm, B. A., Ho, N.-C. & Peacor, D. R. 1994. High-resolution X-ray texture goniometry. *J. Struct. Geol.* **16**, 1029–1032.

van der Pluijm, B. A. & Kaars-Sijpesteijn, B. H. 1984. Chlorite-mica aggregates: Morphology, orientation, development and bearing on cleavage formation in very low-grade rocks. *J. Struct. Geol.* **6**, 399–407.

Wenk, H.-R. 1985. Measurement of pole figures. In: *Preferred Orientation in Deformed Metals and Rocks: An Introduction to Modern Texture Analysis* (edited by Wenk, H.-R.). Academic Press, New York.

Wood, D. S. 1974. Current views on the development of slaty cleavage. *Am. Rev. Earth Planet. Sci.* **2**, 369–401.